A CMOS Implementation of FitzHugh–Nagumo Neuron Model

Bernabé Linares-Barranco, *Student Member, IEEE*, Edgar Sánchez-Sinencio, *Senior Member, IEEE*, Angel Rodríguez-Vázquez, *Member, IEEE*, and José L. Huertas, *Member, IEEE*

Abstract—**A complete derivation of neuron model is presented, starting with the description of the fundamental biological mechanisms involved in the living neural cell, followed by the mathematical model formulation extracted from these mechanisms, and a circuit theory technique to obtain a physical IC suitable circuit that emulates the derived mathematical equations culminating with the presentation of the experimental results of a chip fabricated in a 2-μm double-metal, double-poly CMOS process. It is emphasized that the FitzHugh–Nagumo model is very adequate for emulation of small biological systems. A reduced complexity oscillatory model suitable for implementation of relatively large neural network architectures is also introduced with several corresponding CMOS realizations and measured results.**

I. Introduction

SEVERAL neural network algorithms have been proposed in recent years that successfully replicate some of the properties of the brain, such as learning, associative memory, image or speech recognition, feature extraction, and pattern classification [1]–[6]. All of these algorithms are based on extremely simplified artificial neuron models. They are usually modeled by static nonlinear input–output relationships, some of them called *sigmoidal functions*. However, it is well known that biological neurons have a more complex input–output behavior. Living neurons fire a train of output pulses when the spatial and temporal summation of all the incoming signals exceeds a certain threshold (reference) value. On the other hand, it is also common knowledge that for a proper operation of the present neural network algorithms, it is not necessary to use too complex neuron models, not even resembling biological-like neurons. Nevertheless, it is not clear that with the simple neuron models that have been used so far in engineering and computer science that it would be possible to implement, artificially, all the brain-type functions of living beings. A simple sophistication introduced in neural modeling by several researchers is to make the neuron outputs oscillatory [7]–[13]. This means that the output of a neuron becomes a sequence of pulses provided that the spatial and temporal summation of the incoming signals exceeds a certain threshold. Otherwise, no output pulses occur. The immediate application of these oscillatory neurons is in the emulation of small biological neural circuits whose behavior has been well studied by physiologists [14]. The works of Ryckebusch *et al.* [8] and Koch and Brunner [10] are examples of the use of artificial oscillatory neurons for the emulation of small biological neural circuits. Another interesting application for pulsed neural networks is in the control of electrical motors as recently proposed [15].

In this paper we are presenting a CMOS implementation of a very well known and studied mathematical model of oscillating biological neurons, namely the FitzHugh–Nagumo model [16], which is a simplification of a more realistic model proposed by Hodgkin and Huxley [17]. We believe that for a good understanding of Hodgkin–Huxley's model (and therefore, of FitzHugh–Nagumo's model) an insight into the phenomena that take place in the living neural cell is absolutely necessary. It is this reasoning that has motivated us to include a whole section (Section II) to describe the physiology behind the biological neuron and the corresponding derivation of the model. In Section III this model is simplified, and the resulting mathematical equations are used to generate a suitable IC circuit that emulates these equations. Section IV is devoted to the presentation of the experimentally measured results of a prototype fabricated in a 2-μm double-metal, double-poly CMOS process (thanks and through MOSIS). In Section V we present further simplifications of the previous models, called hysteresis-based models, which are more suitable for neural network architecture implementations with their corresponding measured results from fabricated CMOS prototypes.

Manuscript received December 10, 1990; revised March 13, 1991.

B. Linares-Barranco is with the Department of Electrical Engineering, Texas A&M University, College Station, TX 77843 and the Universidad de Sevilla, 41012 Seville, Spain.

E. Sánchez-Sinencio is with the Department of Electrical Engineering, Texas A&M University, College Station, TX 77843.

A. Rodríguez-Vázquez and J. L. Huertas are with the Facultad de Física, Universidad de Sevilla, 41012 Seville, Spain.

IEEE Log Number 9100256.

0018-9200/91/0700-0956$01.00 ©1991 IEEE

II. Physiology of the Biological Neuron

In this section we are going to describe briefly the biological mechanisms [18], [19] involved in the interaction between neurons and how, as a consequence of this interaction, a neuron generates an electrical impulse that is called the *action potential*. A neuron is a living cell immersed in an interstitial fluid. There exists a voltage difference between the inside and the outside of the cell that is produced by an unequal distribution of electrolytes inside and outside of the cell membrane. This unequal distribution of ions is a consequence of the cell membrane having different permeability factors for each of the ions. For the time being, assume that inside the cell membrane there are K^+ ions and large organic A^- ions, while outside there are mainly Cl^- and Na^+ ions. The cell membrane is always impermeable to the A^- ions so that they always remain inside the cell. During the resting state the cell membrane is permeable only to K^+ and Cl^- ions. Since the membrane is permeable to K^+ and Cl^- ions, K^+ will tend to diffuse outwards, while Cl^- will tend to diffuse inwards. As a consequence of this diffusion, an electrical field will be produced (negative inside with respect to the outside) that opposes the diffusion of ions down their concentration gradient. An equilibrium state will be established in which the force of the electrical field against the ions equals the chemical force that makes the ions diffuse. At this equilibrium state, typically, a voltage difference of 60–80 mV is present between the internal and external walls of the cell membrane, called *membrane potential*.

The cell membrane is impermeable to Na^+ in the resting state of the neuron, for which the resting potential is approximately -75 mV (inside with respect to outside). However, the Na^+ permeability factor of the membrane can be made nonzero, and this is what happens when the neuron cell is producing its *action potential*. If the permeabilities of the membrane change, then the voltage drop V_m between inside and outside of the cell changes according to the following Goldman equation [19]:

$$V_m = 58\ \text{mV} \log \frac{P_K[K^+]_{\text{out}} + P_{Na}[Na^+]_{\text{out}} + P_{Cl}[Cl^-]_{\text{in}}}{P_K[K^+]_{\text{in}} + P_{Na}[Na^+]_{\text{in}} + P_{Cl}[Cl^-]_{\text{out}}} \tag{1}$$

where P_K, P_{Na}, and P_{Cl} are the relative membrane permeabilities for K^+, Na^+, and Cl^-, respectively, $[K^+]_{\text{out}}$, $[Na^+]_{\text{out}}$, and $[Cl^-]_{\text{out}}$ are the concentrations of ions K^+, Na^+, and Cl^- outside the membrane, and $[K^+]_{\text{in}}$, $[Na^+]_{\text{in}}$, and $[Cl^-]_{\text{in}}$ are the concentrations inside. During the resting state of the neuron (when $P_{Na} = 0$) $V_m \simeq -75$ mV, but at the peak of the action potential (when P_{Na} is maximum) $V_m \simeq +50$ mV. During every action potential there is a flow of Na^+ inwards the cell, that increases the membrane voltage, followed by a flow of K^+ outwards to reestablish the resting state potential. Naturally, there is a mechanism that, after the action potential, is going to pump Na^+ outside, and K^+ inside, so that the resting concentrations of these ions are recovered. This is performed independently by the so-called Na^+–K^+ pumps. They are very complex organic molecules that literally pump Na^+ out and K^+ in against their concentration gradients, by means of a sequence of chemical metabolic reactions that consume energy.

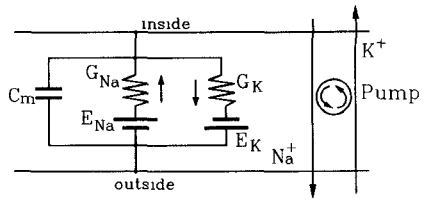

Fig. 1. Equivalent electrical circuit for electrical properties of the nerve membrane.

At this point we can give an equivalent electrical circuit for the electrical properties of the nerve membrane, where the different permeability factors are represented by conductances G_{Na} and G_K. Several channels have been identified so far, each for a different ion, but we are going to concentrate only on two of them, the Na^+ and the K^+ channels. (Later we will also mention the Cl^- channels.) The circuit is shown in Fig. 1 where the capacitance C_m imparted by the lipids of the membrane has been included. E_K is the resting potential of the neuron (75 mV) and E_{Na} is the voltage to which the action potential tends during its rising stage (50 mV). At the resting state $G_{Na} \simeq 0$, but at the peak of the action potential $G_{Na} \gg G_K$.

Inside the cell membrane there are embedded the so-called ionic channels, which are physical channels that can be opened and closed by different stimuli, and when open allow the flux of certain ions. The opening and closing of these channels is what changes the permeability of the membrane, and therefore, the membrane potential.

A. The Na^+ Channels

We are going to consider only two different types of Na^+ channels: the ones opened by organic molecules called *neurotransmitters* released by the end of a synapse when it receives an electrical impulse, and the ones that are opened when the membrane voltage reaches a certain threshold (approximately -50 mV).[1]

1) The Chemically Gated Channel: When an electrical impulse reaches the end of an excitatory synapse (which is separated from the next neural cell by a *synaptic cleft* of 20–40 nm), excitatory neurotransmitters are released into the synaptic cleft. These are molecules that bind temporarily to these chemically gated Na^+ channels (also called neuroreceptors). These neuroreceptors are proteins built into the structure of the membrane, which have the property of changing their structural geometry when a neurotransmitter binds to it, opening an ionic gate and hence changing the permeability and increasing G_{Na}. After a few milliseconds the neurotransmitters are hydro-

[1]Recent studies [19] reveal that there are also some intermediate types of channels, i.e., they can be opened by the two mechanisms.

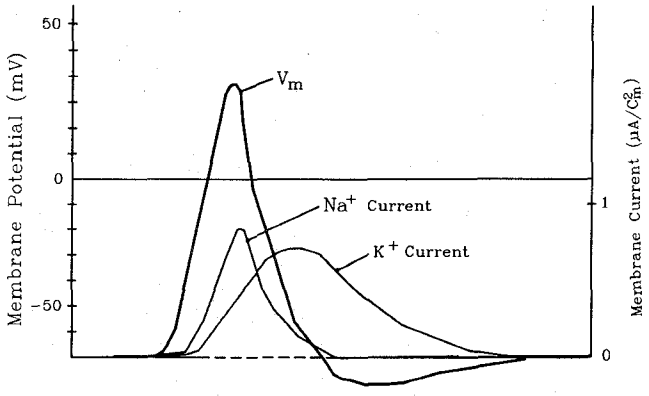

Fig. 2. Membrane voltage and ionic currents during an action potential in a cell membrane.

lyzed into inactive products that are recycled into the synapse and converted again to neurotransmitters for future use.

2) The Voltage-Gated Channel: This channel is another protein that consists of four equal rigid units of 300 amino acids that are joined by other chains of flexible amino acids. These four units are arranged in a cyclindrical fashion inside the membrane. If the four segments are close enough no channel is present, but if they separate (no more than 5 Å) a Na^+ channel is available. Some regions of the protein are charged positively and others negatively. It is believed that interactions between these oppositely charged regions serve as sensors of changes in transmembrane voltage, producing changes in the configuration of the channel protein, which opens the channel slightly allowing flow of Na^+. Such channels remain open only for a few milliseconds, and their flow of ions can be represented by a square pulse of current (1 to 2 pA) of the same amplitude for all active channels but with different widths. By summing all the currents of these channels the total Na^+ current of the cell membrane, shown in Fig. 2, is obtained. If the amount of chemically gated channels that have been opened is high enough so that the threshold voltage of the voltage-gated channels is reached, they will open and hence further increase the membrane potential so that more and more channels will open. A chain reaction is thus produced that makes the Na^+ conductivity very high during a few milliseconds. The transient membrane voltage V_m produced under these conditions is called the action potential (see Fig. 2). The amplitude and shape of this action potential are characteristic of the cell and do not depend on the signals that triggered it.[2]

B. The K^+ Channel

There are several types of K^+ channels, but the action of all of them is to stabilize the membrane potential to the resting voltage. Their effect can be summarized as a current opposite to the Na^+ one that is activated after some delay by an increase in the membrane voltage as shown in Fig. 2. Since this current produces a decrease in membrane potential, it will make, after the peak of the Na^+ current, the voltage to reach its resting value. Furthermore, if originally not enough Na^+ channels were opened fast enough, this K^+ current will start to make the membrane potential decrease before the threshold voltage is reached and, therefore, abort the action potential.

When the chemically gated Na^+ channels were mentioned, it was affirmed that they were opened by excitatory neurotransmitters released by excitatory synapses. There are also inhibitory neurotransmitters that are released when an electrical impulse reaches an inhibitory synapse. These neurotransmitters open Cl^- channels and therefore make the internal voltage of the cell even more negative, so that a stronger excitation will be needed to trigger the action potential. Thus, the Cl^- channels tend to counterbalance the Na^+ channels. An electric circuit modeling all the activity produced by the action potential in a neural cell is depicted in Fig. 3.

I_e represents the triggering current produced by the opening of the (excitatory) chemically gated Na^+ channels, while I_i is the current of the Cl^- channels opened through the inhibitory synapses. The axons of the neural cells are also represented in Fig. 3 as distributed *RC* lines.[3] They allow the propagation of the electrical impulses to neighboring neurons. It is worthwhile to mention here that action potentials can be produced in any living cell if properly excited. The action potential is a property of any cell membrane. What makes the cells of the nervous system unique in this sense is that they are able to propagate action potentials through axons and synaptic connections to other cells.

The part of the circuit of Fig. 3 enclosed by broken lines is very similar to the one that Hodgkin and Huxley proposed in 1952 [17] to relate the current and voltage through the nervous cell membrane during an action potential. They gave mathematical expressions for the different conductances, which were governed by time- and voltage-dependent differential equations. The model of Hodgkin and Huxley explains very well the generation of the action potential, but it fails to explain the generation of more than a single impulse, such as the complex firing patterns that characterize most neurons [19]. These patterns can be explained, however, by the presence of other types of ionic channels in the membrane. Their global effect is similar to allowing the Na^+ channels to remain open as long as the membrane voltage is above the threshold that opens them. In the following section, we will consider a simplification of Hodgkin and Huxley's model by FitzHugh and Nagumo [16], [21] where the Na^+

[2]If the signal that triggered the action potential is strong enough, even though the amplitude of action potentials remains constant, a train of action potentials will be produced. The number of action potentials and the separation between them depend on the strength of the input.

[3]More precisely, the axons should be modeled as a distributed line of elements like the circuit comprised by broken lines in Fig. 3. Such a distributed line is able to regenerate the action potential along its way to the next synaptic connection without degrading it.

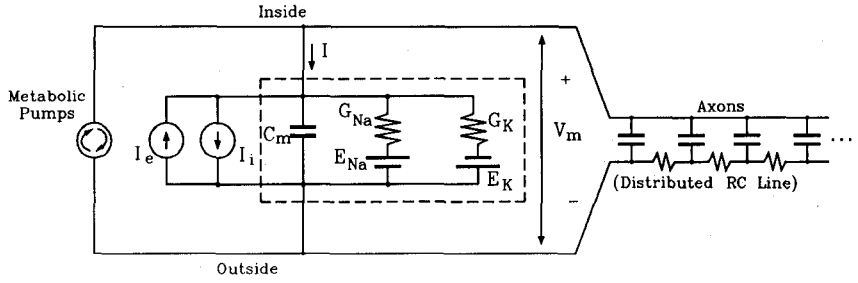

Fig. 3. Electrical circuit model that explains the generation of the action potential in a neural cell.

conductance is only voltage dependent (but not time dependent) and, therefore, is able to model the generation of trains of pulses. In the circuit of Fig. 3 we have included a current source that represents the Na^+–K^+ pump. This current should not be considered as forming part of an electrical circuit that explains the generation of action potentials, because this pump works independently of the action potential and its function is only to avoid accumulation of Na^+ ions inside the cell and of K^+ ions outside. Also, the load of the *RC* line can be neglected for practical purposes. This is a distributed line of elements, like the circuit comprised by broken lines in Fig. 3, that will propagate the action potential by regenerating it.

Another aspect we would like to mention before ending this section is how to model the synaptic interconnection between neurons. Remember that when an electric impulse reaches the end of a synapse, a certain amount of neurotransmitters is released into the spacing between this synapse and the cell membrane (synaptic cleft) of the next neuron. These neurotransmitters remain in the synaptic cleft for a few milliseconds and open some of the chemically gated Na^+ (or Cl^-) channels. The more excitatory neurotransmitters are released, the more chemically gated channels will be opened and the more likely it is that the membrane voltage will reach the threshold that opens the voltage-gated Na^+ channels. The more inhibitory neurotransmitters are released, the more negative the membrane voltage will become and the less likely the threshold will be reached. For each neuron that is receiving neurotransmitters from all the synapses connected to it, a spatial and a temporal summation of all the inputs is performed. Spatial in the sense that each synapse is contributing to increase (if excitatory) or decrease (if inhibitory) the membrane voltage when it receives an electrical impulse, and temporal because the more electrical impulses arrive the more neurotransmitters are released before there is time to inactivate them (for further recycling) and a higher variation in membrane voltage is achieved. This can be modeled by the circuit of Fig. 4, where all the synaptic inputs are algebraically summed (spatial summation) at a certain time and this sum is fed through a lossy integrator (temporal summation) whose output determines the total excitation current $(I_e - I_i)$ for the neuron. The voltages $V_1, V_2, \cdots, V_n$ are the membrane voltages of all the neurons that connect through axons and synapses to the destination neuron of Fig. 3. Observe

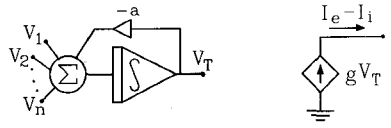

Fig. 4. Diagram for modeling all of the synaptic connections to one neuron.

that a is the feedback term that makes the integrator lossy.[4]

III. Fitzhugh–Nagumo Neuron Model and Circuit Implementation

The simplifications introduced by FitzHugh and Nagumo in the circuit comprised by broken lines in Fig. 3 are a different modeling of the Na^+ and K^+ conductances. Since the Na^+ current is a fast current that strongly depends on the membrane voltage, it is modeled by a time-independent nonlinear conductance as shown in Fig. 5.

On the other hand, the K^+ current is a slow current that does not depend very nonlinearly on the membrane voltage. Therefore, G_K in Fig. 3 is modeled by a linear resistor R connected in series with an inductor L and a voltage source V_0 that represents the membrane's resting potential as shown in Fig. 6. It should be emphasized that the model discussed here is very simple in comparison with the Hodgkin–Huxley one.

This model is mathematically described by the following set of first-order differential equations:

$$C_m \frac{dV_m}{dt} = I - i_K - f_{Na}(V_m) \tag{2a}$$

$$L \frac{di_K}{dt} = V_m + V_0 - Ri_K. \tag{2b}$$

In this paper we propose a CMOS circuit implementation of this set of equations. The circuit of Fig. 6 is not suitable for a direct CMOS implementation due to the presence of L. We will use a transconductance-mode technique to implement these equations directly because of its versatility to implement linear and nonlinear [20] systems. Consider a general system of N nonlinear first-

[4]The feedback term a makes $V_T(t) \to 0$ when $\Sigma_{i=1}^n V_i = 0$.

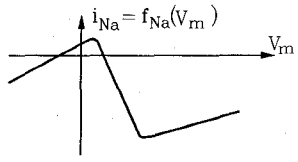

Fig. 5. Na^+ current as a function of membrane potential in the simplified model proposed by FitzHugh and Nagumo.

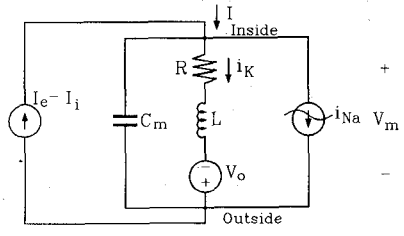

Fig. 6. Equivalent circuit for FitzHugh–Nagumo neuron model.

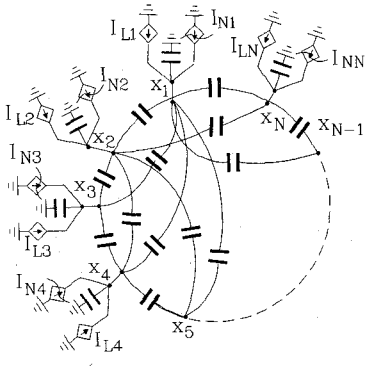

Fig. 7. General topology representing N nonlinear differential equations.

order differential equations in the variables $x_1, x_2, \cdots, x_N$:

$$y_{oj} + \sum_{i=1}^{N} g_{ij}x_i + f_j(\vec{x}) + \sum_{i=1}^{N} B_{ij}\dot{x}_i = 0, \qquad j = 1, \cdots, N \tag{3}$$

y_{oj}, g_{ij}, and B_{ij} being constant parameters and $f_j(\cdot)$ nonlinear functions of $x_1, x_2, \cdots, x_N$.

This system of equations is realized by the circuit of Fig. 7. It consists of N nodes of voltage x_j. Each node j is connected to ground through a capacitor C_{jj} and to each other node i by a capacitor C_{ij}. Two current sources I_{Lj} and I_{Nj} are also connected to each node j. I_{Lj} is linearly dependent on the node voltages of all the other nodes:

$$I_{Lj} \triangleq \sum_{i=1}^{N} g_{ij}x_i + y_{oj} \tag{4}$$

where g_{ij} (which can be positive or negative) is the transconductance relating interaction between nodes i and j and y_{oj} is an offset term. I_{Nj} is a nonlinearly dependent current source:

$$I_{Nj} = f_j(x_1, x_2, \cdots, x_N) = f_j(\vec{x}). \tag{5}$$

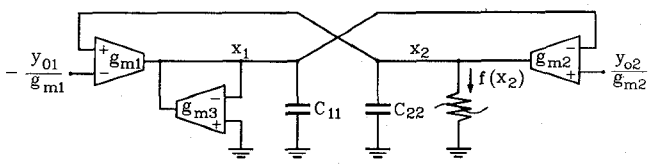

Fig. 8. Transconductance-mode implementation of FitzHugh–Nagumo's equations.

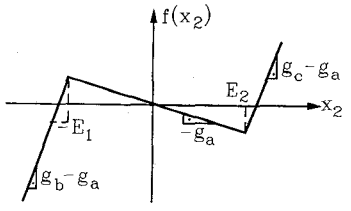

Fig. 9. N-shaped piecewise linear function for nonlinear element.

For each node j the following KCL equation holds:

$$y_{oj} + \sum_{i=1}^{N} g_{ij}x_i + f_j(\vec{x}) = \sum_{i=1}^{N} C_{ij}(\dot{x}_j - \dot{x}_i) + C_{jj}\dot{x}_j. \tag{6}$$

If we define now

$$B_{ij} \triangleq \begin{cases} C_{ij}, & \text{if } i \neq j \\ -\sum_{l=1}^{N} C_{jl}, & \text{if } i = j \end{cases} \tag{7}$$

(3) is obtained.

By comparing (2) and (3) the particular circuit for FitzHugh–Nagumo's model can be identified from Fig. 7. The resulting circuit is shown in Fig. 8.

This circuit solves the following equations:

$$C_{22}\dot{x}_2 = y_{o2} - g_{m2}x_1 - f(x_2) \tag{8a}$$

$$C_{11}\dot{x}_1 = y_{o1} + g_{m1}x_2 - g_{m3}x_1 \tag{8b}$$

which can be identified with (2) by making

$$V_m = x_2, \quad i_K = x_1, \quad I = \frac{y_{o2}}{g_{m2}}, \quad V_0 = \frac{y_{o1}}{g_{m1}},$$

$$C_m = \frac{C_{22}}{g_{m2}}, \quad L = \frac{C_{11}}{g_{m1}}, \quad R = \frac{g_{m3}}{g_{m1}}, \quad f_{Na}(V_m) = \frac{f(x_2)}{g_{m2}}. \tag{9}$$

The exact form of the function $f(\cdot)$ seems not to be very critical. Originally, a cubic polynomial [16] for Fig. 5 was suggested, but a piecewise linear dependence can give the same basic properties to the system [21]. We will consider $f(\cdot)$ as shown in Fig. 9, which can be implemented by the circuit depicted in Fig. 10 [20].

A phase portrait of the equilibrium points of the system described by (8) is shown in Fig. 11, where $g_b - g_a = g_c - g_a = g_l$. The equilibrium points are obtained when $\dot{x}_1 = \dot{x}_2 = 0$. Since there is a nonlinearity with three linear

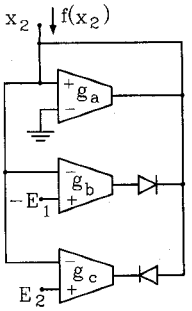

Fig. 10. Implementation of the nonlinear function using transconductance-mode techniques. x_2 and $f(x_2)$ represent a voltage and a current variable, respectively.

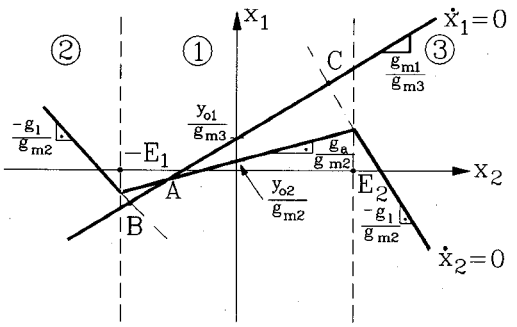

Fig. 11. Phase portrait of the system characterized by (8).

segments, we can divide the phase plane into three linear regions, namely, regions ①, ②, and ③ as shown in Fig. 11. For region ① the state equations are given by

$$\begin{bmatrix}\dot{x}_1\\ \dot{x}_2\end{bmatrix}=\begin{bmatrix}-\dfrac{g_{m3}}{C_{11}} & \dfrac{g_{m1}}{C_{11}}\\ -\dfrac{g_{m2}}{C_{22}} & \dfrac{g_a}{C_{22}}\end{bmatrix}\begin{bmatrix}x_1\\ x_2\end{bmatrix}+\begin{bmatrix}\dfrac{y_{o1}}{C_{11}}\\ \dfrac{y_{o2}}{C_{22}}\end{bmatrix}. \tag{10}$$

An equilibrium point is called *real* if it is located inside the linear region that defines it, and therefore, can be reached by the system. An equilibrium point is called *virtual* if it is located outside the linear region that defines it, and therefore, will never be reached by the system because as it approaches it the linear region will change and also the corresponding equilibrium point. The equilibrium point A of region ① is real because, as shown in Fig. 11, it is inside region ①. This point will be unstable [22] if the trace and determinant of (10) satisfy

$$T_0=\frac{g_a}{C_{22}}-\frac{g_{m3}}{C_{11}}>0$$

$$\Delta_0=\frac{g_{m1}g_{m2}}{C_{11}C_{22}}-\frac{g_a g_{m3}}{C_{11}C_{22}}>0. \tag{11}$$

For regions ② and ③ we can describe the behavior of the system by

$$\begin{bmatrix}\dot{x}_1\\ \dot{x}_2\end{bmatrix}=\begin{bmatrix}-\dfrac{g_{m3}}{C_{11}} & \dfrac{g_{m1}}{C_{11}}\\ -\dfrac{g_{m2}}{C_{22}} & \dfrac{-g_l}{C_{22}}\end{bmatrix}\begin{bmatrix}x_1\\ x_2\end{bmatrix}+\begin{bmatrix}\dfrac{y_{o1}}{C_{11}}\\ \dfrac{y_{o2}-\alpha(g_l+g_a)}{C_{22}}\end{bmatrix} \tag{12}$$

where $\alpha=-E_1$ for region ② and $\alpha=+E_2$ for region ③. Note that the equilibrium points B and C for regions ② and ③, respectively, are virtual in Fig. 11. B and C will be stable if [20]

$$T_1=\frac{-g_l}{C_{22}}-\frac{g_{m3}}{C_{11}}<0$$

$$\Delta_1=\frac{g_{m1}g_{m2}}{C_{11}C_{22}}+\frac{g_l g_{m3}}{C_{11}C_{22}}>0. \tag{13}$$

For proper operation of the system we need to make A unstable and B and C stable equilibrium points. If the system is at a certain time in region ①, since A is unstable it will move away from it until the system eventually reaches either region ② or ③. When this happens, since the equilibrium point (B or C) is stable, the system will be attracted by it. But before it is reached, the system will find itself again in region ① and repelled by A. As a consequence of all this, the system will oscillate in a limited cycle in which it goes from regions ② to ③ and vice versa crossing region ① each time. Also note that in Fig. 11 the relative positions of the curves $\dot{x}_1=0$ and $\dot{x}_2=0$ can be varied by changing y_{o1} and/or y_{o2}, and therefore, B and C can be made real equilibrium points. If either B or C is real, the system will reach the stable equilibrium point and stay there. This situation corresponds to the resting state of the neuron where no action potentials are generated. But if y_{o1} or y_{o2} is changed beyond the threshold value that makes either B or C change from real to virtual, the system will start to produce oscillations (the neuron is active and firing action potentials). Note that (see (9)) y_{o2} represents the total excitation current I_e-I_i of Figs. 3 and 6, but in this case, we can change either y_{o2} or y_{o1} because the effect is the same.

IV. Experimental Results

The IC prototype of Fig. 8 was fabricated in a standard 2-μm double-metal, double-poly CMOS process (through and thanks to MOSIS). The OTA's employed were linearized ones [23]. The diodes were implemented using diode-connected MOS transistors. When the two external inputs y_{o1} and y_{o2} are set to zero, the outputs of the circuit are free-running oscillations. If the time constants of the two differential equations in (8) are made very different, i.e., $g_{m1}/C_{11}\ll g_{m2}/C_{22}$, then FitzHugh–Nagumo's equations simulate the behavior of biological cell membranes. The corresponding measured response

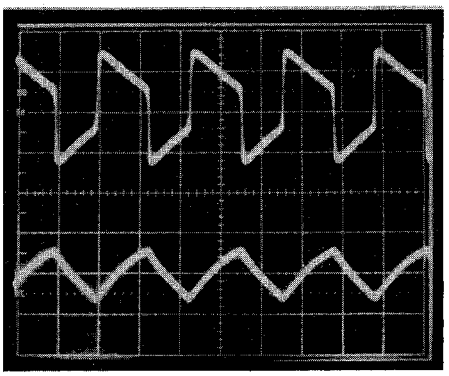

Fig. 12. Free-running oscillations of oscillator of Fig. 8 when $g_{m1}/C_{11} \ll g_{m2}/C_{22}$.

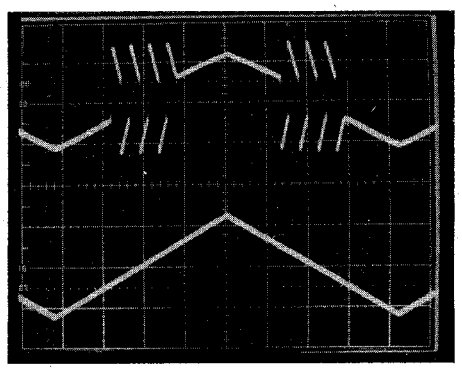

Fig. 13. Input–output relation of oscillator of Fig. 8. Lower trace: input (y_{o2}); upper trace: output (x_2).

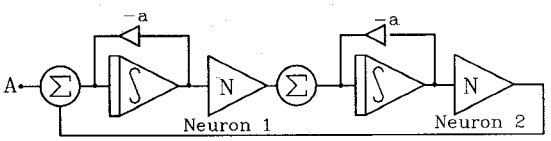

Fig. 14. Connection of two oscillatory neurons in a loop.

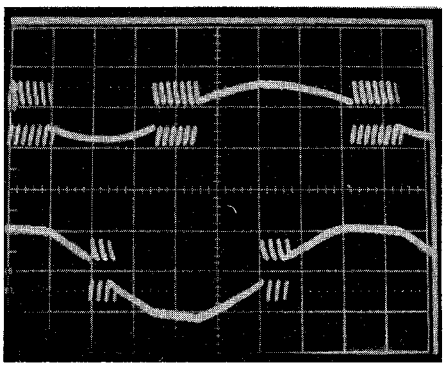

Fig. 15. Steady response of a two-neuron-loop oscillator when $A = 0$.

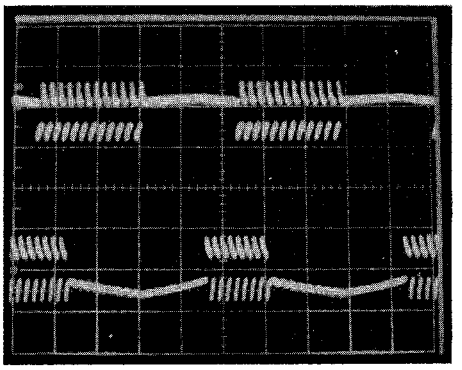

Fig. 16. Temporarily stable pattern observed when A is such that the two-neuron loop is chaotic.

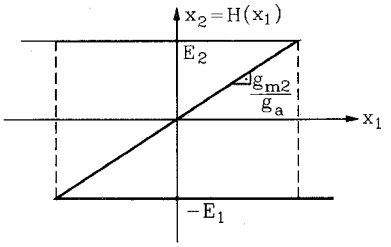

Fig. 17. Hysteresis transfer function extracted from FitzHugh–Nagumo's model.

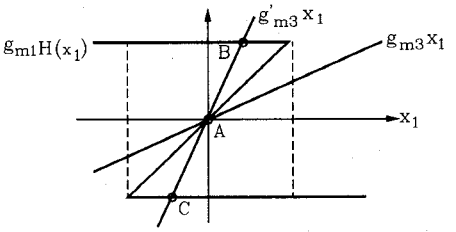

Fig. 18. Equilibrium points of the hysteretic system.

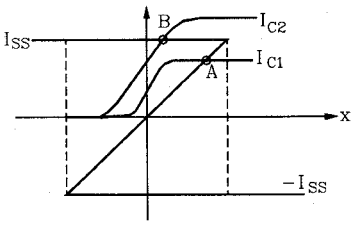

Fig. 19. Equilibrium points of the modified hysteretic system.

of the circuit for this case is shown in Fig. 12. When signal y_{o2} is considered as the input to the neuron and x_2 as its output, we can see in Fig. 13 the measured input–output relationship of the cell (y_{o1} was arbitrarily set to zero), where y_2 is the lower trace and x_2 is the upper trace. Note that, as can be seen in Fig. 13, the circuit can model the behavior of a double-threshold neuron: if the input signal is either above the upper threshold or below the lower one, no oscillations are produced. But if the input y_{o2} is between the two thresholds, the output is a firing sequence of pulses. This effect can be anticipated by examining Fig. 11. Note that by increasing y_{o2}, equilibrium point C will become real and oscillations will disappear. On the other hand, by decreasing y_{o2}, B will become real and no oscillations will be produced.

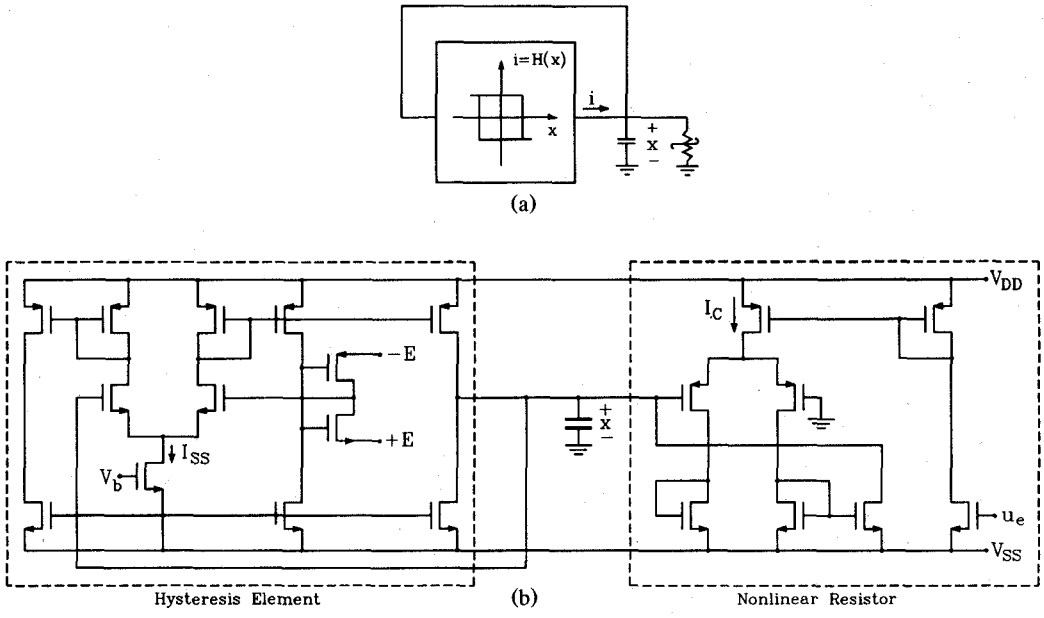

Fig. 20. CMOS circuit for modified hysteretic neuron cell. (a) Block diagram. (b) Transistor-level implementation (all transistors are minimum size).

A. Loop of Two FitzHugh–Nagumo Neurons

Using the interconnection principle of Fig. 4 we interconnected two FitzHugh–Nagumo cells as shown in Fig. 14, using two neurons of Fig. 8 and two lossy integrators. When $A = 0$ the response is stable, as is shown in Fig. 15. But for certain values of A the signals observed at the output change randomly between different oscillation patterns. One of these temporary patterns can be seen in Fig. 16. This might be an out-of-synchronization phenomenon, which has been shown to have a chaotic nature [24].

V. Simpler Oscillatory Neuron Models

The motivation to develop simpler models (but still keeping the oscillatory nature) is based on their potential use [13] in implementing hardware for neural network architectures. The free-running oscillator of FitzHugh–Nagumo's system can be further simplified to a hysteresis oscillator if, in (8), we impose the following conditions:

$$\begin{aligned} g_c - g_a = g_b - g_a \to \infty \text{ in } f(x_2) \\ y_{o1} = y_{o2} = 0 \\ \frac{g_{m1}}{C_{11}} \ll \frac{g_{m2}}{C_{22}} \to \infty \end{aligned} \tag{14}$$

The consequence of this is that the first equation in (8) will reach its steady state immediately (in comparison to the second equation). Therefore, the first equation can be reduced to

$$x_1 = -\frac{f(x_2)}{g_{m2}}. \tag{15}$$

Taking the inverse of (15) yields

$$x_2 = H(x_1) \tag{16}$$

which is a hysteretic transfer function, as depicted in Fig. 17.

Hence, (8) simplifies into

$$H(x_1) - g_{m1}x_1 - \frac{C_{11}}{g_{m1}}\dot{x}_1 = 0. \tag{17}$$

The equilibrium points of this system ($\dot{x}_1 = 0$) are given by the intersection of the two curves in Fig. 18.

If $(g_{m1}g_{m2})/g_a > g_{m3}$, the only equilibrium point is A, which is unstable according to the analysis in Section III. In this case, (17) represents an oscillator. But, if $(g_{m1}g_{m2})/g_a < g_{m3}$, there are two more equilibrium points B and C which are stable, and then no oscillations are present. Therefore, the oscillator can be turned on and off by changing g_{m3}. A circuit implementation of a system similar to this has already been presented by the authors in [25]. For a CMOS implementation, however, it is easier to substitute the linear resistor g_{m3}^{-1} by a nonlinear one as shown in Figs. 19 [26] and 20.

If $I_C < I_{SS}$, the equilibrium point A is unstable and the circuit will oscillate. If $I_C > I_{SS}$, B is stable and no oscillations are obtained. The hysteresis element is built with a conventional operational transconductance amplifier that has a double output. One of them is connected to its positive input terminal and to a pair of diode-connected MOS transistors. The diodes are connected to two bias voltages $+E$ and $-E$. This positive feedback causes the amplifier to saturate so that the output current, through the two outputs, is either $+I_{SS}$ or $-I_{SS}$. The width of the hysteresis loop is controlled by the bias voltages $+E$ and $-E$. The second output of the transconductance amplifier is the actual output of the hysteresis element, while its negative input terminal is the input to the hysteresis device. The output of the hysteresis element is connected to the integrating capacitor and to a nonlinear resistor.

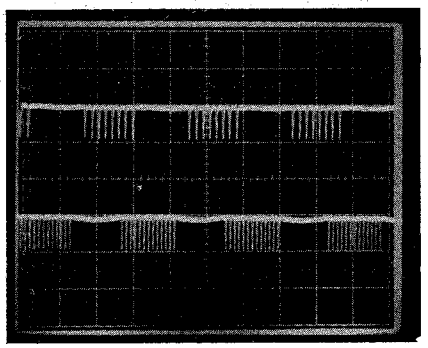

Fig. 21. Pattern generation by a loop of two hysteretic neural cells.

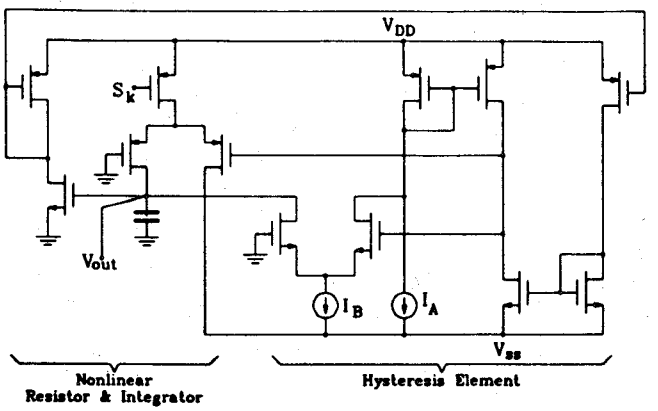

Fig. 22. Current-mode implementation of the block diagram of Fig. 20(a).

This nonlinear resistor sinks a constant current I_C if $x > 0$ and performs as an open circuit if $x < 0$. This operation is done with a differential pair so that only the current through one of its branches is directed to the input, as shown in Fig. 20(b). The parameters that can be adjusted in the neural oscillator of Fig. 20 are I_{SS} and $\pm E$. E controls the amplitude of the oscillations at $x(t)$, and I_{SS} controls the slope of the triangular waveforms. Both of them can be used to change the frequency of the oscillations. This simple neural oscillator was fabricated in a 3-μm double-metal CMOS process [26] and two of them were interconnected using the same arrangement shown in Fig. 14. The network was able to generate the patterns shown in Fig. 21.

VI. Conclusions

We have introduced a CMOS circuit that emulates the FitzHugh–Nagumo neuron model. The use of this model implementation is mainly intended for biological system emulations. It is conceivable that knowledge obtained from experiences interconnecting several of these artificial neurons can help to improve the understanding of interactions of biological neurons.

In the field of hardware implementation of neural network paradigms, the use of artificial neurons based on the FitzHugh–Nagumo model will not, for some time yet, be practical due to the large silicon area. This is due to the fact that at least hundreds or thousands of neurons are required in the implementation of practical neural network architectures.[5] At the same time, the oscillatory neuron type [7]–[15] has the potential to implement artificial neural networks that can mimic biological neural networks more closely and consequently it is expected that these implementations will have better properties and performance than neural networks using artificial neurons not resembling the biological neurons at all. Thus, to be able to use an oscillatory neuron model for large neural network architectures a trade-off is in order. This trade-off involves accuracy (or fidelity) in representing the biological neuron versus simplicity (complexity) of the circuit implementation [8], [9], [13]. We have already introduced a simplified version of a neuron model as illustrated in Fig. 20. One step further can be taken by using the implementation of the compact circuit shown in Fig. 22, where all transistors are minimum size [11]. This last oscillatory neuron implementation uses current as the signal processing instead of voltage and provides more convenient properties and performance than voltage-mode circuits. As a matter of comparison, the basic neuron implementations of Figs. 8, 20, and 22 occupy approximately 230×10^3 μm^2, 44×10^3 μm^2, and 14×10^3 μm^2, respectively. However, the circuit complexity, and fidelity to mimic the biological neuron are different for the several existent applications. The concept of using frequency information, rather than voltage, seems promising as discussed in [13] and [15]. Furthermore, the company, General Dynamics, has recently presented a "general-purpose neural IC" where frequency is used to characterize synapses weights. In brief, we can state that oscillatory neuron models have a wide range of applications for biological neuron emulations as well as in hardware of neural network architectures.

[5]However, complex tasks may require only a few tens of neurons. For instance, the recognition of handwritten digits can be performed with only 45 neurons [27].

Acknowledgment

The authors would like to thank the unknown reviewers as well as Dr. A. Tsay and Prof. R. Newcomb for valuable comments on the manuscript.

References

[1] G. A. Carpenter and S. Grossberg, "A massively parallel architecture for a self-organizing neural pattern recognition machine," *Comput. Vision, Graphics, Image Processing*, vol. 31, pp. 54–115, 1987.

[2] D. W. Tank and J. J. Hopfield, "Simple 'neural' optimization networks: An A/D converter, signal decision circuit, and linear programming circuit," *IEEE Trans. Circuits Syst.*, vol. CAS-33, no. 5, pp. 533–541, May 1986.

[3] J. A. Anderson, J. N. Silverstein, S. A. Ritz, and R. S. Jones, "Distinctive features, categorical perception, and probability learning: Some applications of a neural network," *Psychol. Rev.*, vol. 84, pp. 413–451, 1977.

[4] D. E. Rumelhart, G. E. Hinton, and R. J. Williams, "Learning internal representations by error propagation," in *Parallel Distributed Processing: Explorations in the Microstructures of Cognition*,

vol. 1, D. E. Rumelhart and J. L. McClelland, Eds. Cambridge, MA: MIT Press, 1986, pp. 318–362.
[5] T. Kohonen, *Self-Organization and Associative Memory*. New York: Springer-Verlag, 1988.
[6] B. Kosko, "Adaptive bidirectional associative memories," *Appl. Opt.*, vol. 26, no. 23, pp. 4947–4960, Dec. 1, 1987.
[7] M. Savigny, G. Moon, N. El-Leithy, M. Zaghloul, and R. W. Newcomb, "Hysteresis turn-on–off voltages for a neural-type cell," in *Proc. IEEE Int. Symp. Circuits Syst.* (Helsinki, Finland), June 1988, vol. 2, pp. 993–996.
[8] S. Ryckebusch, J. M. Bowes, and C. Mead, "Modeling small oscillating biological networks in analog VLSI," in *Neural Information Processing Systems 1 (NIPS)*, D. S. Touretzki, Ed. San Mateo, CA: Morgan Kaufmann, 1989, pp. 384–393.
[9] P. Chintrakulchai, N. Nintunze, A. Wu, and J. Meador, "A wide-dynamic-range programmable synapse for impulse neural networks," in *Proc. IEEE Int. Symp. Circuits Syst.* (New Orleans, LA), May 1990, vol. 4, pp. 2975–2977.
[10] U. T. Koch and M. Brunner, "A modular analog neuron-model for research and teaching," *Biol. Cybern.*, vol. 59, pp. 303–312, 1988.
[11] B. Linares-Barranco, E. Sánchez-Sinecio, and A. Rodríguez-Vázquez, "CMOS circuit implementations for neuron models," in *Proc. IEEE Int. Symp. Circuits Syst.* (New Orleans, LA), May 1990, vol. 3, pp. 2421–2424.
[12] J. E. Tomberg and K. K. K. Kaski, "Pulse-density modulation technique in VLSI implementations of neural network algorithms," *IEEE J. Solid-State Circuits*, vol. 25, no. 5, pp. 1277–1286, Oct. 1990.
[13] A. F. Murray, D. Del Corso, and L. Tarassenko, "Pulse-stream VLSI neural networks mixing analog and digital techniques," *IEEE Trans. Neural Networks*, vol. 2, pp. 193–204, Mar. 1991.
[14] A. I. Selverston, *Model Neural Networks and Behavior*. New York: Plenum, 1985.
[15] S. DeWeerth, L. Nielsen, C. Mead, and K. D. Astran, "A simple neuron servo," *IEEE Trans. Neural Networks*, vol. 2, pp. 248–251, Mar. 1991.
[16] R. FitzHugh, "Impulses and physiological states in theoretical models of nerve membrane," *Biophys. J.*, vol. 1, 1961.
[17] A. L. Hodgkin and A. F. Huxley, "A qualitative description of membrane current and its application to conduction and exictation in nerves," *J. Phys.*, vol. 177, pp. 500–544, 1952.
[18] F. L. Straud, *Physiology. A Regulatory Systems Approach*. New York: MacMillan, 1978.
[19] G. M. Shepherd, *Neurobiology*. New York: Oxford University Press, 1988.
[20] E. Sánchez-Sinencio, J. Ramírez-Angulo, B. Linares-Barranco, and A. Rodríguez-Vázquez, "Operational transconductance amplifier based nonlinear function syntheses," *IEEE J. Solid-State Circuits*, vol. 24, no. 6, pp. 1576–1586, Dec. 1989.
[21] J. P. Keener, "Analog circuitry for the Van der Pol and FitzHugh–Nagumo equations," *IEEE Trans. Syst., Man., Cybern.*, vol. SMC-13, no. 5, Sept./Oct. 1983.
[22] L. O. Chua, C. A. Desoer, and E. S. Kuh, *Linear and Nonlinear Circuits*. New York: McGraw-Hill, 1987.
[23] A. P. Nedungadi and R. L. Geiger, "High-frequency voltage-controlled continuous-time lowpass filter using linearized CMOS integrators," *Electron. Lett.*, vol. 22, pp. 729–731, June 1986.
[24] Y. S. Tang, A. I. Messand, and L. O. Chua, "Synchronization and chaos," *IEEE Trans. Circuits Syst.*, vol. CAS-30, no. 9, pp. 620–626, Sept. 1983.
[25] B. Linares-Barranco, E. Sánchez-Sinencio, A Rodríguez-Vázquez, and J. L. Huertas, "A programmable neural oscillator cell," *IEEE Trans. Circuits Syst.*, vol. 36, no. 5, pp. 756–761, May 1989.
[26] B. Linares-Barranco, E. Sánchez-Sinencio, R. W. Newcomb, A. Rodríguez-Vázquez, and J. L. Huertas, "A novel CMOS analog neural oscillator cell," in *Proc. IEEE Int. Symp. Circuits Syst.* (Portland, OR), June 1989, vol. 1, pp. 794–797.
[27] P. Y. Alla, G. Sancier, S. Kuerr, L. Personnaz, and G. Dreyfus, "Design and implementation of a dedicated neural network for handwritten digit recognition," presented at the IFIP Workshop Silicon Architectures for Neural Nets, St. Paul de Vence, France, 1990.

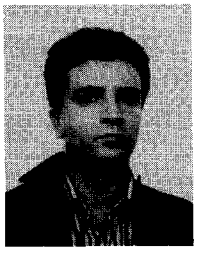

Bernabé Linares-Barranco was born in Granada, Spain, on November 26, 1962. He did his elementary studies in Germany until 1973. He received the B.Sc. degree in electronic physics in June 1986, the M.S. degree in microelectronics in September 1987, and the Ph.D. degree in microelectronics in June 1990, all of them from the University of Seville, Spain.

Since May 1988 he has been with the Department of Electrical Engineering, Texas A&M University, College Station, where he is working towards his second Ph.D. degree. His research interests are in the area of nonlinear analog and neural networks microelectronic design.

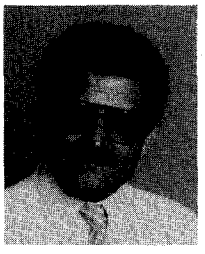

Edgar Sánchez-Sinencio (S'72–M'74–SM'83) received the M.S.E.E. degree from Stanford University, Stanford, CA, and the Ph.D. degree from the University of Illinois at Champaign-Urbana, in 1970 and 1973, respectively.

In 1974 he was with the Center Research Laboratories, Nippon Electric Company, Ltd., Japan. From 1976 to 1983 he was the Head of the Department of Electronics at the National Institute of Astrophysics, Optics and Electronics, Puebla, Mexico. Currently, he is with Texas A&M University, College Station, as a Professor. He is the co-author of *Switched-Capacitor Circuits* (Van Nostrand-Reinhold, 1984). His interests are in the area of solid-state circuits, including CMOS neural network implementations and computer-aided circuit design.

Dr. Sánchez-Sinencio was the General Chairman of the 1983 26th Midwest Symposium on Circuits and Systems. He has been Associate Editor for *IEEE Circuits and Systems Magazine* (1982–1984), for *IEEE Circuits and Device Magazine* (1985–1988), for the IEEE TRANSACTIONS ON CIRCUITS AND SYSTEMS (1985–1987), and for the IEEE TRANSACTIONS ON NEURAL NETWORKS (1990–). He is currently the President of the IEEE Circuits and Systems Technical Committee on Neural Systems and Application, and a member of the IEEE CAS Board of Governors.

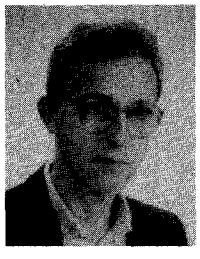

Angel Rodríguez-Vázquez (M'80) received the Licenciado en Física degree in 1977, and the Doctor en Ciencias Físicas degree in 1983, both from the University of Seville, Spain.

Since 1978 he has been with the Departamento de Electrónica y Electromagnetismo at the Universidad de Sevilla, where he is currently employed as an Associate Professor. His research interest lies in the fields of analog/digital integrated circuit design, analog integrated neural and nonlinear networks, and modeling of analog integrated circuits.

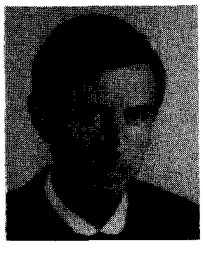

José L. Huertas (M'74) received the Licenciado en Física degree in 1969, and the Doctor en Ciencias Físicas degree in 1973, both from the University of Seville, Spain.

From 1970 to 1971 he was with the Philips International Institute, Eindhoven, The Netherlands, as a Postgraduate Student. Since 1971 he has been with the Departamento de Electrónica y Electromagnetismo at the Universidad de Sevilla, where he is currently employed as a Professor. His research interest lies in the fields of multivalued logic, sequential machines, analog circuit design, and nonlinear network analysis and synthesis.